Nanosecond Optical Rotatory Dispersion Spectroscopy: Application to Photolyzed Hemoglobin-CO Kinetics

Daniel B. Shapiro, Robert A. Goldbeck, Diping Che, Raymond M. Esquerra, Sarah J. Paquette, and David S. Kliger
Department of Chemistry and Biochemistry, University of California at Santa Cruz, Santa Cruz, California 95064 USA

ABSTRACT A standard technique for static optical rotatory dispersion (ORD) measurements is adapted to the measurement of ORD changes on a nanosecond (ns) time scale, giving approximately a million-fold improvement in time-resolution over conventional instrumentation. The technique described here is similar in principle to a technique recently developed for ns time-resolved circular dichroism (TRCD) spectroscopy, although the time-resolved optical rotatory dispersion (TRORD) technique requires fewer optical components. As with static ORD, TRORD measurements may be interpreted by empirical comparisons or may be transformed, via the Kramers-Kronig relations, to more easily interpreted TRCD spectra. TRORD can offer experimental advantages over TRCD in studying kinetic processes effecting changes in the chiral structures of biological molecules. In particular, the wider dispersion of ORD bands compared with the corresponding CD bands means that ORD information may often be obtained outside of absorption bands, a signal-to-noise advantage for multichannel measurements. Demonstration of the technique by its application to ns TRORD and the transform-calculated TRCD of carboxy-hemoglobin (Hb-CO) after laser photolysis is presented.

INTRODUCTION

Before the advent of modern circular dichroism (CD) instrumentation based on photoelastic modulators and phase sensitive detection, the structural properties of chiral molecules were commonly studied using optical rotatory dispersion (ORD), the rotation of the plane of polarization of linearly polarized light by the circular birefringence (CB) of a chiral chromophore measured as a function of wavelength (Djerassi, 1960). Among the methods used in such static ORD studies was a technique due to Keston and Lospalluto (1953), implemented in the Beckman DU spectrophotometer as the Standard Model D Keston polarimetric attachment (Gallop, 1957; Poulsen, 1960; Rabinovitch and Yamakawa, 1979). In the present work, we describe a novel apparatus for time-resolved ORD (TRORD) that incorporates the quasi-null optical method of Keston and Lospalluto into a ns laser photolysis apparatus to achieve a million-fold improvement in ORD time-resolution over conventional instruments.

Several years ago, an ellipsometric technique for ns time-resolved CD (TRCD) spectroscopy was developed in this laboratory to study dynamic structural changes in chiral biological macromolecules (Lewis et al., 1985). We have since applied this technique to a variety of biological systems, including hemoglobin (Lewis et al., 1985; Björling, 1991), myoglobin (Milder et al., 1988), tRNA (Milder et al., 1989), cytochrome aa_3 (Goldbeck et al., 1991), cytochrome ba_3 (Goldbeck et al., 1992), and phytochrome (Björling et al., 1992; Chen et al., 1993), as well as several inorganic complexes (see Lewis et al., 1992, for references). The TRCD technique is quasi-null; the quantity measured is the differential change in transmission of a highly eccentric, elliptically polarized probe beam through a crossed analyzing polarizer that is induced by the circularly dichroic sample. More recently, we have also developed a ns time-resolved linear dichroism (TRLD) apparatus based on a quasi-null optical approach, in this case using nearly-crossed linear polarizers (Che et al., 1994). This optical method is in fact identical to the ORD method of Keston and Lospalluto (1953). As a Mueller matrix analysis shows, both LD and CB (or optical rotation) will be detected by this approach (Che et al., 1994). Thus, TRLD can be monitored in time-dependent, anisotropic, achiral systems, e.g., a symmetric chromophore after phototransformation (by a linearly polarized laser) and before rotational reorientation has extinguished photoselection-induced LD. Furthermore, because the LD induced by phototransformations can be several orders of magnitude larger than the magnitudes typically encountered for natural CB ($<10^{-3}$), it should often be possible to measure TRLD to a good approximation in chiral systems as well. On the other hand, and most important for the present work, at times after complete rotational reorientation, the method will be uniquely sensitive to the TRORD of time-dependent, isotropic, chiral systems, e.g., dissymmetric, phototransformed chromophores. In addition, we show that an appropriate orientation of the polarization optics to minimize the photoselection-induced LD ensures that TRORD is detected without significant interference from the LD even at early times before rotational reorientation is complete.

The present work introduces a ns implementation of the quasi-null TRORD technique with a Mueller calculus description of the optical principles used and a description of the ns laser-photolysis ORD apparatus. The feasibility of the technique is demonstrated with an application to a biological system, ligand-photolysis intermediates of carbonmonoxy

Received for publication 11 July 1994 and in final form 12 October 1994.
Address reprint requests to Dr. David S. Kliger, Department of Chemistry and Biochemistry, University of California, Santa Cruz, CA 95064. Tel.: 408-459-2106; Fax: 408-459-2935; E-mail: Kliger@chemistry.ucsc.edu.

0006-3495/95/01/326/09 $2.00

hemoglobin (HbCO), showing the ability of ns TRORD to resolve the kinetics of multiple processes. (A more complete Mueller analysis, including artifacts associated with optical imperfections in TRLD/ORD measurements, has been given previously (Che et al., 1994).) The signal-to-noise advantage of TRORD over TRCD (see Discussion) is exploited in the present HbCO study to obtain, with practical amounts of signal averaging, ns chiral spectral data that approach ordinary absorption spectra in the quality of its signal-to-noise ratio (peak S/N $\geq$ 100). Such a level of quality is necessary if time-resolved chiroptical data are to support a global kinetic analysis yielding lifetimes and amplitudes for spectral intermediates associated with structural changes in proteins. Although the main purpose of this paper is to introduce a potentially powerful technique to study changes in chiral structures with nanosecond resolution, we also offer a preliminary interpretation of the TRORD results, presented here for hemoglobin in light of recent TRCD results (S. C. Björling, S. J. Paquette, S. J. Milder, R. A. Goldbeck, and D. S. Kliger, unpublished data).

QUASI-NULL MEASUREMENT OF OPTICAL ROTATORY DISPERSION

The measurement of CB using the quasi-null method of Keston and Lospallutos (1953) may be understood in terms of a Mueller matrix analysis. The polarization of light in a classical wave description is given by the direction of the electric field vector, **E**. Thus, the intensity and polarization state of light is fully described by the four elements of the Stokes vector,

$$\mathbf{I}_s = \begin{bmatrix} I \\ Q \\ U \\ V \end{bmatrix} = \begin{bmatrix} E_h^2 + E_v^2 \\ E_h^2 - E_v^2 \\ E_+^2 - E_-^2 \\ E_r^2 - E_l^2 \end{bmatrix}, \tag{1}$$

where v, h, $+$, $-$, r, and l refer to the vertical linear, horizontal linear, positive diagonal linear, negative diagonal linear, and right and left circular polarization components for light of arbitrary polarization, respectively, and I, Q, U, and V are the total intensity, the difference of vertical and horizontal polarized intensities, the difference of diagonal intensities, and the difference of the circularly polarized intensities, respectively.

The effect of the optical properties of a substance or optical element on the Stokes vector can be written in terms of the Mueller matrix,

$$\mathbf{M} = \begin{bmatrix} M_{11} & M_{12} & M_{13} & M_{14} \\ M_{21} & M_{22} & M_{23} & M_{24} \\ M_{31} & M_{32} & M_{33} & M_{34} \\ M_{41} & M_{42} & M_{43} & M_{44} \end{bmatrix}, \tag{2}$$

which operates on the Stokes vector to produce a new vector describing the transformed light in terms of its polarization and intensity.

TRORD measurements are performed in our lab using a polarized actinic beam produced by a laser and an initially unpolarized probe beam produced by a flash lamp. The sample is placed between two near-crossed probe polarizers.

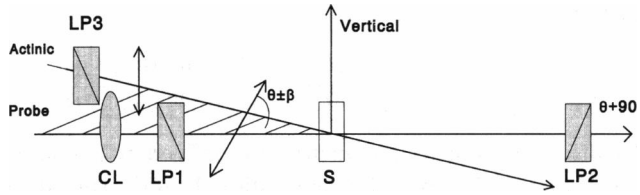

FIGURE 1 Schematic diagram of the TRORD instrument. An actinic laser beam intersects the lamp probe beam at an arbitrary angle. The probe beam passes though a collimating lens (CL) and the probe polarizer (LP1) oriented along $\theta \pm \beta$ before traversing the sample (S). A second probe polarizer (LP2) oriented along $\theta + 90°$ analyzes the beam before detection. A laser polarizer (LP3) ensures pure vertical polarization of the actinic beam. Vertical is defined as normal to the plane formed by the probe and actinic beams.

A schematic diagram representing the measurement is shown in Fig. 1. Let the vertical direction be defined as normal to the plane defined by the actinic and probe beams. The unpolarized light produced by the probe lamp is described by the normalized Stokes vector [1, 0, 0, 0]. The Mueller matrix for a polarizer has the general form

$$\mathbf{P} = \frac{1}{2}\begin{bmatrix} 1 & \cos 2\theta & \sin 2\theta & 0 \\ \cos 2\theta & \cos^2 2\theta & \cos 2\theta \sin 2\theta & 0 \\ \sin 2\theta & \cos 2\theta \sin 2\theta & \sin^2 2\theta & 0 \\ 0 & 0 & 0 & 0 \end{bmatrix}, \tag{3}$$

where θ is the angle of the polarizer. The measurement may be conducted such that the polarizers are initially set at θ = 0 and 90° with respect to horizontal (positive θ being defined in a clockwise direction when looking toward the probe source). Hereafter, this geometry (with the polarizers initially set in the horizontal and vertical directions) will be referred to as geometry 1. The first polarizer is rotated either clockwise or counter-clockwise by a small angle designated by β. The Stokes vector for the light after transmittance through the first polarizer and sample is calculated as

$$\begin{bmatrix} M_{11} & M_{12} & M_{13} & M_{14} \\ M_{21} & M_{22} & M_{23} & M_{24} \\ M_{31} & M_{32} & M_{33} & M_{34} \\ M_{41} & M_{42} & M_{43} & M_{44} \end{bmatrix} \tag{4}$$

$$\times \frac{1}{2}\begin{bmatrix} 1 & \cos 2\beta & \sin 2\beta & 0 \\ \cos 2\beta & \cos^2 2\beta & \cos 2\beta \sin 2\beta & 0 \\ \sin 2\beta & \cos 2\beta \sin 2\beta & \sin^2 2\beta & 0 \\ 0 & 0 & 0 & 0 \end{bmatrix}\begin{bmatrix} 1 \\ 0 \\ 0 \\ 0 \end{bmatrix}$$

$$= \frac{1}{2}\begin{bmatrix} M_{11} + M_{12}\cos 2\beta + M_{13}\sin 2\beta \\ M_{21} + M_{22}\cos 2\beta + M_{23}\sin 2\beta \\ M_{31} + M_{32}\cos 2\beta + M_{33}\sin 2\beta \\ M_{41} + M_{42}\cos 2\beta + M_{43}\sin 2\beta \end{bmatrix}$$

After the second polarizer, the total intensity is given by

$$I(\beta) = \{M_{11} + M_{12}\cos 2\beta + M_{13}\sin 2\beta\} - \{M_{21} + M_{22}\cos 2\beta + M_{23}\sin 2\beta\} \tag{5}$$

The quantity of interest is the difference of the intensities

measured at $\pm\beta$ divided by their sum,

$$s = \frac{I(\beta) - I(-\beta)}{I(\beta) + I(-\beta)} = \frac{(M_{13} - M_{23})\sin 2\beta}{M_{11} - M_{21} + (M_{12} - M_{22})\cos 2\beta} \quad (6)$$

An alternate geometry (geometry 2) is defined by a rotation of the two initial probe polarizer positions by 45° so that their initial positions are diagonal. A measurement conducted using geometry 2 results in the quantity of interest, s', given by

$$s' = \frac{I(\beta) - I(-\beta)}{I(\beta) + I(-\beta)} = \frac{(M_{32} - M_{12})\sin 2\beta}{M_{11} - M_{31} + (M_{13} - M_{33})\cos 2\beta} \quad (7)$$

For a thin sample, where differential absorptions are very small compared to the total absorption, the Mueller matrix can be written (Jensen et al., 1978)

$$\mathbf{M} = e^{-A}\begin{bmatrix} 1 & -LD & -LD' & CD \\ -LD & 1 & CB & LB' \\ -LD' & -CB & 1 & -LB \\ CD & -LB' & LB & 1 \end{bmatrix}, \quad (8)$$

where

$$A = \frac{\ln 10(A_h + A_v)}{2},$$

$$LB = \frac{2\pi(n_h - n_v)l}{\lambda}, \qquad LB' = \frac{2\pi(n_+ - n_-)l}{\lambda},$$

$$LD = \frac{\ln 10(A_h - A_v)}{2}, \qquad LD' = \frac{\ln 10(A_+ - A_-)}{2}, \quad (9)$$

$$CB = \frac{2\pi(n_l - n_r)l}{\lambda}, \qquad CD = \frac{\ln 10(A_l - A_r)}{2},$$

A denotes an absorbance, LB refers to linear birefringence, and λ, n, and l are the wavelength of light, index of refraction and path length of the sample. In general, the elements of the matrix in Eq. 8 substituted into Eq. 6 or 7 give the measured quantity, a combination of LD and CB. Thus, in geometry 1, when β is small, s becomes

$$\frac{I(\beta) - I(-\beta)}{I(\beta) + I(-\beta)} \approx \frac{-(LD' + CB)\sin 2\beta}{1 - \cos 2\beta} \cong \frac{-(LD' + CB)}{\beta}, \quad (10)$$

and in geometry 2,

$$\frac{I(\beta) - I(-\beta)}{I(\beta) + I(-\beta)} \cong \frac{LD - CB}{\beta}. \quad (11)$$

In both geometries, $-CB$ is measured. However, the two geometries measure linear dichroism between different (orthogonal) directions. Each quantity is measured by taking the difference of transmitted intensities when the first probe polarizer is rotated $\pm\beta$. These rotations introduce a bit of diagonal light in geometry 1 and horizontal or vertical light in geometry 2. Thus, in geometry 1 (defined by initial horizontal and vertical orientations of the probe polarizers), LD' (between the diagonal directions) is measured. In geometry 2 (defined by initial crossed diagonal orientations of the probe polarizers), LD (between the horizontal and vertical directions) is measured.

In many applications, including the present one, a sample can be oriented by photoselection or other means. In such cases, linear dichroism can be quite large, dominating the measured ORD. However, if there is no preferred orientation to molecules in the sample, LD will be zero and one can accurately measure ORD. Moreover, in many situations, an appropriate choice of the polarization optics can ensure that LD or LD' are negligible. If the polarization of the photolysis beam is vertical and measurements are conducted using geometry 1, then LD' is zero and Eq. 10 becomes

$$s = \frac{I(\beta) - I(-\beta)}{I(\beta) + I(-\beta)} \cong \frac{-CB}{\beta}. \quad (12)$$

A detailed analysis of the artifacts arising from optical imperfections that may affect measurements of ORD has been given by Che et al. (1994).

MATERIALS AND METHODS

The TRORD instrument is represented in Fig. 1. It is very similar to the TRCD instrument described previously (Lewis et al., 1985; Lewis et al., 1992; Kliger et al., 1990). A Xenon flash lamp produces unpolarized light that is collimated with a lens. The light is polarized by the initial Glan-Thompson polarizer, which is rotated by the small angles $\pm\beta$ from the horizontal position (β = 0.011 was used here). The actinic beam, produced by a Quanta Ray DCR-11 Nd:YAG laser, frequency-doubled to 532 nm, was typically operated at a repetition rate of 2 Hz, had a laser power adjusted to 17 mJ per pulse and beam diameter of about 7 mm. A cleanup polarizer ensured the purity of the vertical polarization of the actinic beam. A second, vertical, Glan-Thompson polarizer was placed after the sample. The extinction between the polarizers was about 10^{-6}. The collimated beam was focused through a 250 μm slit into a Jarrel Ash spectrograph (150 gratings per mm) and detected with a EG&G OMA II detector. A Stanford Instruments DG535 delay/pulse generator was used to control the timing of the detector gate and the firing of the flash lamp with respect to the laser pulse.

The two probe polarizers were aligned so that they were oriented along the horizontal and vertical directions and the laser cleanup polarizer was aligned along the vertical. This alignment was optimized by minimizing the photoinduced LD of a suspension of the purple membrane from the bacteria *Halobacterium halobium* at about 450 μs after laser excitation. This sample has a large photoinduced LD at this time compared to CB (Che et al., 1994).

Hemoglobin A was prepared as described previously (Geraci et al., 1969). Whole blood was washed in 1% NaCl. The cells were lysed by bathing them in a large volume of distilled water. The membranes were removed by centrifugation, and the supernatant containing the purified Hb A was dialyzed against distilled water and then pelleted and frozen for storage. At the time of measurement, the Hb A was diluted to 120 μM (in heme) in 0.1 M sodium phosphate buffer, pH 7.3. Less than 100 μM sodium dithionite was added to the hemoglobin solution (degassed in CO) to scavenge any traces of oxygen. During the measurements, the hemoglobin solution was maintained in a CO atmosphere and flowed through a 1/2 mm path-length cell.

ORD was measured at 43 times after laser photolysis from 100 ns to 40 ms. Hb-HbCO absorption difference measurements, using a polarizer set to the magic angle, were measured at identical times as the ORD measurements with identical gate sizes. The gate of the OMA detector was varied from 100 ns (at early times) to 2.5 μs (at later times). Data were collected from about 300–700 nm with a resolution of about 4 nm. ORD measurements were

performed on three separate hemoglobin samples. A total of 8950 ORD measurements were averaged for each early time point using a 100 ns detector gate, 2304 measurements were averaged for intermediate times using a 1 μs gate, and 1536 measurements were averaged for later times using a 2.5 μs gate.

The averaged TRORD data were smoothed using a 15-point (0.6 nm per point) Savitzky-Golay quadratic spectral convolution. The time-resolved absorption (TROD) and TRORD data were baseline-offset to give a null signal between 650 and 700 nm. Data taken between 350 and 550 were then used for further analysis using singular value decomposition (SVD) (Henry and Hofrichter, 1992; Golub and Reinsch, 1970; Brodersen, 1990). The application of SVD involves writing the data in terms of an $m \times n$ matrix, A, which gives the signal (ORD or OD) at each of the m wavelengths and n time delays. The matrix A is decomposed into the product of three matrices:

$$A = USV^T. \tag{13}$$

U is an $m \times n$ matrix containing the signal value for n orthonormal basis spectra at m wavelengths. V^T denotes the transpose of V, an $n \times n$ matrix giving the amplitude of each basis spectrum at the n time delays. S is an $n \times n$ diagonal matrix containing the singular values of A. The kth singular value determines the degree to which the product of the kth basis spectrum and the jth component of the kth amplitude vector contributes to the spectrum measured at the jth time point. Only the r basis spectra with the largest singular values and their time amplitudes are used to describe the data, i.e., the SVD decomposition is truncated after the rth singular value, the higher values being discarded as noise, to give a more concise, noise-filtered representation of the data. The truncated representation of the A matrix is then used to determine lifetimes and amplitudes of exponential decays of the spectra of intermediate species using a (nonlinear) least-square fitting technique known as global analysis (Goldbeck and Kliger, 1993). In this work, the first five basis spectra with the largest singular values, together with their time courses, were used to make the truncated data matrix, A. The intermediate spectra, together with their exponential decay rates and amplitudes, given by global analysis provide information about the kinetic processes of interest.

RESULTS

Fig. 2 *a* shows the ORD spectrum of the well known standard compound, $(+)_{589}$ tris(ethylenediamine) cobalt-(III) (Λ-$[Co(en)_3]^{3+}$), measured on the ns TRORD apparatus. This ORD spectrum agrees well with those reported previously (Huheey et al., 1990). The CD spectrum of the same sample taken using the quasi-null ellipsometric CD method is shown in Fig. 2 *b*. The Kramers-Kronig transformation of the ORD spectrum (shown in Fig. 2 *c*) reproduces the measured CD spectrum well.

The use of different polarization geometries to discriminate between TRORD and TRLD in near-crossed polarizer measurements is demonstrated in measurements on photolyzed hemoglobin using geometries 1 and 2. Fig. 3 *a* shows the ORD spectrum of HBCO at 100 ns after laser photolysis obtained using geometry 1. Fig. 3 *b* shows the results of a measurement on the same sample at the same delay time after photolysis with the two probe polarizers rotated 45° (geometry 2). The ORD spectrum measured in geometry 1 has been magnified 5 times from its measured value for comparison with the measurement using geometry 2. The photoinduced LD is primarily measured in geometry 2 because it is much greater in magnitude than the ORD.

The time-resolved optical difference spectra of transient-HbCO at 43 times after laser photolysis is shown in Fig. 4. The positive peak around 432 nm corresponds to the increased absorption of the transient photolyzed species relative to HbCO. The negative peak, around 417 nm, corresponds to the decrease in absorption of the transient species relative to HbCO. The return of the transient to the initial state (before photolysis) can be seen by the approach of the difference spectra to zero at later times. The transient ORD spectra of photolyzed HbCO (taken at identical times after

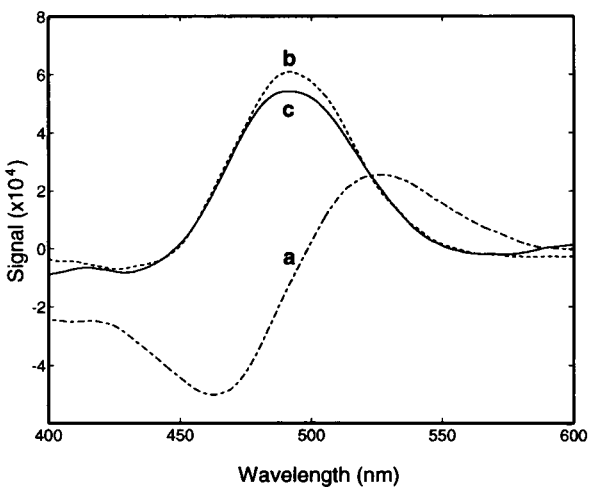

FIGURE 2 ORD and CD of Λ-$[Co(en)_3]^{3+}$. The measurements are plotted according to the definitions of CD and CB given in Eq. 9. The ellipticity and optical rotation (in radians) are CD/2 and CB/2, respectively. (*a*) ORD measured using the near-crossed polarizer technique (– — –). (*b*) CD measured using the ellipsometric technique (– – – –). (*c*) CD obtained using the Kramers-Kronig transformation of the ORD measured spectra (——). All spectra are in arbitrary units.

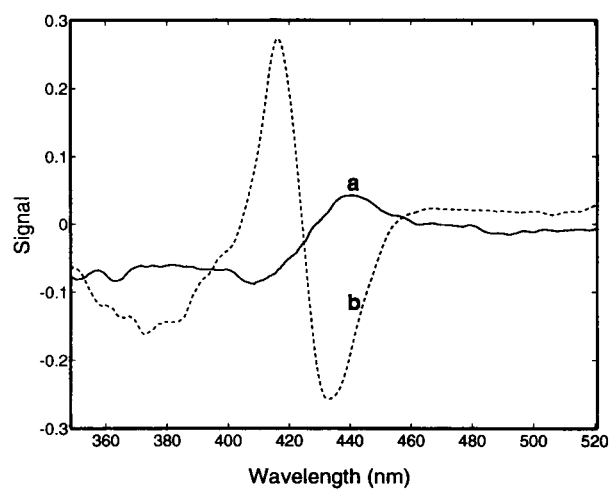

FIGURE 3 TRORD/TRLD measurements with different polarizer geometries discriminate ORD from LD. A 100-ns gate is used to probe intermediates of HbCO 100 ns after photolysis. (*a*) Geometry 1; crossed polarizers are initially oriented along the horizontal and vertical directions to measure the ORD spectrum (——). The signal, given by Eq 12, has been magnified 5 times for comparison with Fig. 3 *b*. On the scale shown, an ORD signal of 0.1 corresponds to a rotation of 0.0063°. (*b*) Geometry 2; crossed polarizers are initially oriented along diagonal directions. The measurement (– – – –) is governed by Eq. 11. A LD signal of 0.3 corresponds to a difference in absorption of 0.0094. Note that the photoinduced LD now dominates the ORD (measured in geometry 1).

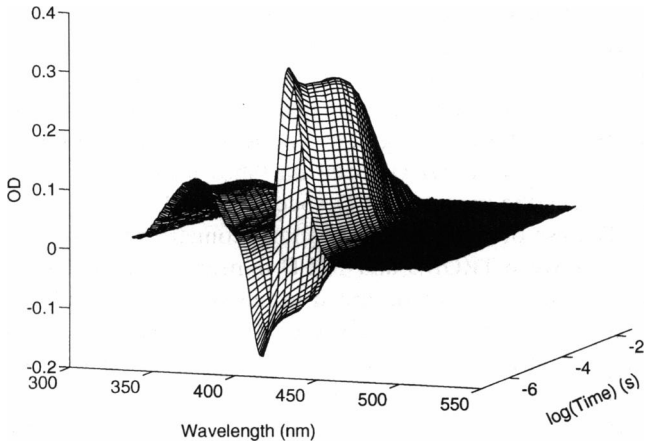

FIGURE 4 TROD of HbCO. The transient Hb-HbCO difference spectrum at 43 time points after photolysis plotted versus wavelength and log(time).

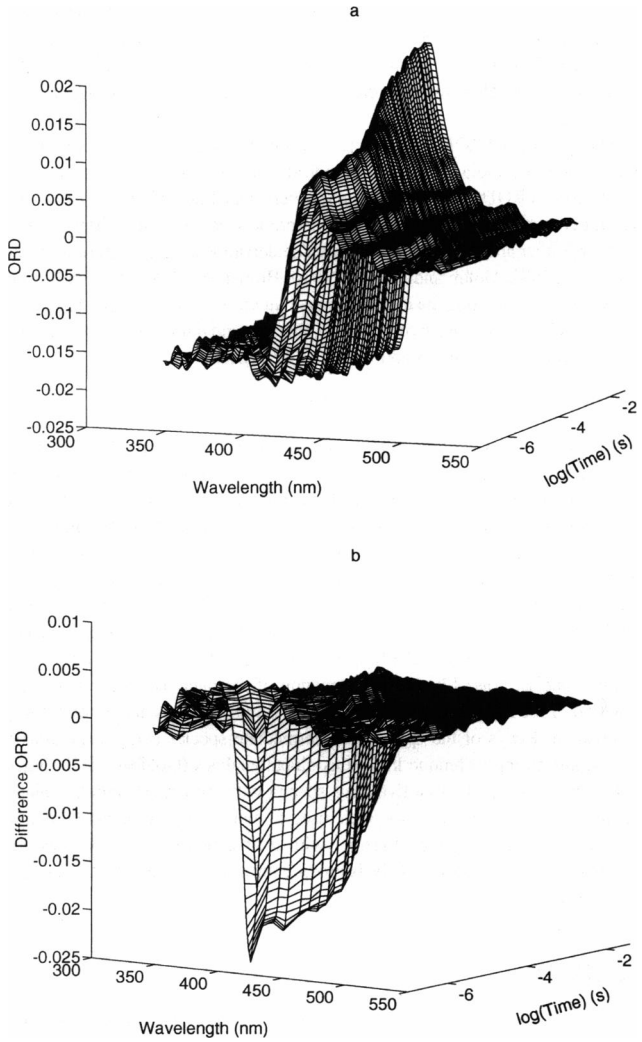

FIGURE 5 TRORD of HbCO. An ORD signal of 0.02 corresponds to a rotation of 0.0063°. (*a*) The transient Hb ORD spectra, as given by Eq. 12, at 43 times after photolysis. (*b*) The difference TRORD of HbCO. The ORD of the unphotolyzed sample was subtracted from each transient.

photolysis as the TROD spectra of Fig. 4) are shown in Fig. 5 *a*. The smaller, red-shifted spectra correspond to those taken at earlier times after photolysis. Fig. 5 *b* shows the transient ORD spectra with the initial ORD spectrum (taken in the absence of photolysis) subtracted from each transient spectrum. These TRORD difference spectra also approach zero for later times, indicating a return to ground state HbCO.

Singular value decomposition (SVD) filtering/compression and global kinetic analysis (of the truncated data matrix) were applied to the TROD data to give apparent lifetimes and amplitudes for the exponential decay of four spectral intermediates, shown in Table 1. (The TROD lifetimes and amplitudes are reported for both a variable gate size and a fixed 10 ns gate. The close similarity of these results shows that the variable gate size used in the TRORD measurements reported here probably did not affect the results of the kinetic analysis.) This multi-exponential analysis implicitly assumes a model in which four species undergo parallel, first-order decays. Although this is not expected to be a realistic picture of photolyzed HbCO, it is a useful and commonly applied model because any kinetic scheme made up of first-order processes will show the same observed decay constants. The amplitudes are model-dependent, however, and are reported here not as representative of concentrations of intermediates, but as rough estimates of the relative importance of each decay constant to the overall spectral kinetics. The TROD lifetimes in Table 1 are similar to those reported previously by Hofrichter et al. (1983) for a four-exponential fit. The lifetimes and amplitudes obtained from analysis of the SVD-filtered TRORD difference spectra shown in Table 1 are quite similar to the TROD results for the two slowest processes, assigned as diffusive rebinding of CO to R state (τ_3) and T state (τ_4) deoxy Hb (Hofrichter et al., 1983). The magnitude of τ_2 is again comparable between the absorption and ORD results, but the amplitude of this process is twice as large in ORD. This process has been assigned to the R $\rightarrow$ T quaternary structure transition, so it is to be expected that the amplitudes reflect the much larger R $-$ T difference observed in the CD/CB of Hb as compared with the R $-$ T absorption difference (Perutz et al., 1974). The most significant difference between the kinetic results for absorption and TRORD arises for the fastest component, τ_1. The ~100 ns time constant found for τ_1 in the TROD has been interpreted in terms of a tertiary relaxation in the region of the hemes, perhaps a final stage in the doming of the heme after photolysis (Spiro et al., 1990). The fastest process observed in the TRORD appears to be 4 times slower than that observed in absorption, with a significantly smaller amplitude. When the TROD measurements taken here are fit to five exponential processes, a new process appears with a small amplitude and a lifetime of about 1 μs (S. J. Paquette, S. C. Björling, R. A. Goldbeck and D. S. Kliger, unpublished data). The TRORD data were too noisy for an independent fit to five exponential processes using global analysis. However, when the TRORD data were forced to fit to the five lifetimes found from TROD, the amplitude obtained for the

TABLE 1 Lifetimes and amplitudes from a four-exponential global kinetic analysis of time-resolved absorption and ORD spectra for photolyzed Hb-CO

	τ_1 (ns)	Amp_1	τ_2 (μs)	Amp_2	τ_3 (μs)	Amp_3	τ_4 (ms)	Amp_4
TROD*	108	0.32	32	0.12	183	0.37	3.7	0.18
TROD‡	114	0.29	28	0.13	166	0.43	3.8	0.16
TRORD*	429	0.20	35	0.22	157	0.36	3.2	0.19

*Sampling gate width varied from 100 ns to 2.5 μs.
‡Constant 10-ns gate.

1 μs process was much greater in TRORD than in TROD. This 1 μs process and the others obtained in a five exponential analysis of TROD, as well as the TRORD amplitudes for these fixed lifetimes, are summarized in Table 2. The normalized TRORD amplitude is 3 times larger than the TROD amplitude for the 1 μs process (process 2 in Table 2).

DISCUSSION

The methods developed in our lab for fast polarization dichroism spectroscopy, ellipsometric TRCD and polarimetric TRLD/ORD, obtain their high sensitivity by using near-crossed polarizers to increase the size of the desired effect relative to the total transmitted intensity. Although, in principle, the highest sensitivity in a measurement of CD, CB, LD, or LB could be achieved with a null measurement using crossed polarizers, this approach does not give sign information and cannot distinguish the four effects when they occur together (the Kramers-Kronig relations show that every CD band has an overlapping ORD and similarly for LD and LB). High sensitivity is retained, sign information is restored, and effective discrimination between optical effects is introduced by using a quasi-null approach. In the TRCD/LB technique, this is accomplished by introducing a small ($\sim 10^{-2}$ radians) linear birefringence, LB′, between the crossed polarizers and modulating its orientation between $\pm 45°$ relative to the polarizer axes, so that the transmitted intensity reflects the total ellipticity induced in the beam by the modulator and sample. The difference signal is proportional to the sum of the CD and the diagonal component of any LB present in the sample, divided by the magnitude of the modulated LB′ to give a roughly 10^2 amplification in relative signal size. This amplification effect gives the quasi-null method a two orders of magnitude S/N advantage over conventional CD methods when considering instrumental noise sources that can be taken as proportional to lamp intensity, such as lamp instability, thermal drift, etc. (the photon shot noise figures of merit for quasi-null and conventional, i.e., modulator LB = 90° and no analyzing polarizer, methods are identical). In addition to discriminating against CB and LD, CD can be further isolated from any photoselection-induced LB present in the sample through the appropriate choice of excitation geometry (Einterz et al., 1985; Björling et al., 1991).

TABLE 2 Lifetimes and amplitudes from a five-exponential global kinetic analysis of time-resolved absorption and the amplitudes obtained from a fit of ORD spectra with these lifetimes held constant, for photolyzed Hb-CO

	Process 1	Process 2	Process 3	Process 4	Process 5
TROD Lifetimes	87 ns	1.0 μs	41 μs	190 μs	3.1 ms
TROD Amplitudes	0.34	0.028	0.12	0.33	0.16
TRORD Amplitudes	0.26	0.11	0.21	0.27	0.15

The quasi-null CB/LD technique is closely analogous to the ellipsometric CD/LB method; as the names suggest, the techniques are related by interchanging the use of circular versus linear polarization elements between the crossed polarizers. Thus, a small circular birefringence (10^{-2} rad) is now modulated between positive and negative orientations, with the transmitted intensity reflecting the total rotation induced in the beam by modulator and sample. (In our implementation, one of the polarizers is rotated instead of adding a separate CB modulator element.) The difference signal is proportional to the sum of the CB and the diagonal component of any linear dichroism (LD′ for geometry 1) present in the sample, divided by the magnitude of the modulated CB to give a 10^2 amplification in relative signal size. This amplification effect again gives the quasi-null approach a S/N advantage over instrumental noise sources in the laser flash photolysis apparatus that is sufficient to achieve ns time resolution with reasonable signal averaging. To complete the analogy, the discrimination against CD and LB inherent in the quasi-null approach is further extended in the case of ORD measurements to photoselection-induced LD discrimination through the appropriate choice of excitation geometry, e.g., alignment of the laser polarization axis with either polarizer axis.

Being related by the Kramers-Kronig relations, CB and CD can be considered the dispersive (real) and absorptive (imaginary) parts, respectively, of the (complex) molecular response function for circularly polarized light, and in principle they contain identical information (Moscowitz, 1962). In practice, however, the localization of CD to the absorption bands of chromophores results in more easily interpreted spectra, and the measurement of CD has generally been preferred over ORD. Although the use of CD largely eclipsed ORD in the 1960's, ORD remains a useful tool for probing chiral structures (Morris, 1990; Akesson and Michelson, 1981; Hanspal and Ralston, 1981; Yip and Sauls, 1992) and its basic physics remains a subject of investigation (Evans, 1990; Evans et al., 1992).

Despite the evident popularity of CD, there are situations where ORD can offer advantages over CD. Experimental

simplicity is one advantage; the elimination of a separate modulator reduces the number of optical elements between the polarizers and thus reduces opportunities for the introduction of artifacts. The broader dispersion of ORD can be another, as in the measurement of optical activity arising from absorption bands beyond the range of direct detection. The dispersion of CB beyond the absorption band-shape can be particularly advantageous for time-resolved spectroscopy, which is often limited by signal-to-noise considerations. This advantage can be seen by taking the absolute value of the signal-to-noise ratios for the CD and ORD bands associated with a simple Gaussian absorption band-shape and integrating this figure of merit over the band. One finds that the integrated S/N is roughly 2 to 4 times larger for ORD, the former factor applying to noise that is proportional to light intensity (e.g., arc wander) and the latter to photon shot noise when the maximum sample absorbance is one. When considering signal averaging with multichannel detection, where an entire spectrum may be obtained with each measurement, this represents about an order of magnitude decrease in the number of averaged measurements required to reach a given level of cumulative signal to noise.

The ORD measured for Λ-$[Co(en)_3]^{3+}$ and HbCO using the ns TRORD apparatus provides experimental confirmation of the principles presented above and confirms the S/N advantages of this approach to ORD spectroscopy. The static ORD of Λ-$[Co(en)_3]^{3+}$ (Fig. 2) demonstrates the ability of the quasi-null Keston-Lospallutos method to accurately measure ORD with a high S/N using the noisy light sources and short sampling times typical of fast kinetic spectroscopy.

As mentioned above, a CD spectrum is usually easier to interpret in terms of molecular parameters than is the corresponding ORD. Thus, it was also important to demonstrate that the method could yield ORD spectra of sufficient quality for transformation (Kramers-Kronig, KK) to accurate CD spectra, at least for favorable cases (nonoverlapping bands). The good agreement of the calculated CD spectrum obtained from a KK transform of the Λ-$[Co(en)_3]^{3+}$ ORD spectrum with the directly measured CD spectrum indicates that TRORD measurements can indeed be a useful source of TRCD spectra, an issue further addressed in the case of HbCO.

The TRORD measurements obtained for photolyzed HbCO demonstrate two points: (1) fast time-resolved ORD spectra can now be obtained with S/N good enough to support a multi-exponential kinetic analysis, and (2) TRORD can be KK transformed to yield calculated TRCD with good accuracy and high S/N for an important case, the Soret bands of hemeproteins. To establish the first point, a standard for comparison and validation of the kinetic analysis of the TRORD results is sought in time-resolved absorption measurements. The kinetic analysis of TRORD and TROD indeed produces closely comparable results for the microsecond through millisecond time regime that encompasses the three slowest observed decay constants, with the difference in amplitudes for the R $\rightarrow$ T rate process (τ_2) being accounted for by the known R $-$ T difference spectra (Perutz et al., 1974). The marked difference found for the fastest time constants and amplitudes appears to be significant and suggests that absorption and ORD are differentially sensitive to different processes occurring in the protein on the submicrosecond time scale. In this regard, TRCD spectra of HbCO measured in the near-UV aromatic bands (S. C. Björling, S. J. Paquette, S. J. Milder, R. A. Goldbeck, and D. S. Kliger, unpublished data) suggests that the first step in a step-wise R $\rightarrow$ T transition, involving conformational changes at the dimer-dimer interfaces, may occur at about 1 μs, in reasonable agreement with the τ_1 found here from TRORD. This hypothesis is also consistent with the small amplitude, 1 μs process found in fitting of HbCO TROD to five exponential processes. (S. J., Paquette, S. C. Björling, R. A. Goldbeck and D. S. Kliger, unpublished data). A high sensitivity of the TRORD measurements to the 1 μs process could explain the lengthening of the fastest TRORD time constant relative to that of TROD in a fit to four exponential processes (429 ns compared with 108 ns). As Table 2 shows, when the TRORD data are forced to fit to the five exponentials obtained by an application of global analysis to TROD, the amplitude of the 1 μs process is greatly increased. In any event, the close similarity of the TRORD kinetic analysis for processes such as CO recombination, which should show identical lifetimes whether measured by absorption or ORD/CD, is convincing evidence for the usefulness of TRORD as a chiral probe of protein dynamics.

In fulfillment of point (2), the TRCD difference spectra (Fig. 6) calculated from a KK transformation of the TRORD data are found to be in good agreement with spectra collected directly in our lab using a ns TRCD instrument (Björling, 1991), with the calculated spectra showing much better S/N than experimental CD spectra obtained under comparable conditions. In the Soret region of the spectrum, changes in both OD and CD (and hence ORD) result from changes in heme ligation and changes in the position of amino acid residues surrounding the heme (Geraci and Parkhurst, 1981). However, the relative sensitivities of OD and ORD to different structural changes and ligation state are expected to be

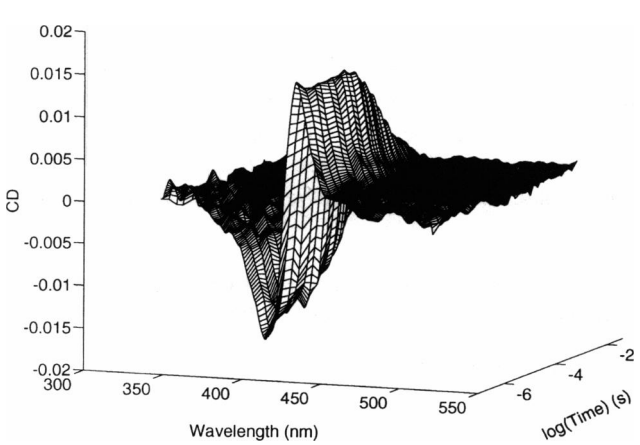

FIGURE 6 TRCD of HbCO. Transient CD difference spectra of HbCO after laser photolysis calculated from the Kramers-Kronig transform of the difference TRORD spectra shown in Fig. 5.

quite different. The Soret CD/ORD arises primarily from dipole-dipole coupling between the hemes and aromatic residues as far as 10–15 Å and, thus, will be sensitive to changes in heme-residue distances and orientations associated with tertiary and quaternary structure changes (Hsu and Woody, 1969, 1971). This suggests that a comparison of kinetics involved in ligand rebinding to Hb obtained in TROD versus TRORD measurements could provide new information about the structure and function of hemoglobin and other proteins, a conclusion that is supported by the divergence in nanosecond spectral kinetics found here for HbCO. In summary, we have demonstrated the ability of the TRORD technique to obtain kinetic information about chiral changes in protein conformation in an application to hemoglobin. The similarities in CO rebinding kinetics found in the TROD and TRORD measurements demonstrate the validity of TRORD as a novel probe of fast protein kinetics. Differences in the early-time kinetics as measured by these two techniques are consistent with their differential sensitivity to protein structure and demonstrate the potential of TRORD to provide new information about protein conformational dynamics. The results and interpretation of the early-time TRORD measurements presented here are necessarily preliminary and are the subject of current efforts in our laboratory. Of primary significance from this current work is the demonstration that this TRORD technique can produce high quality spectral data suitable for detailed kinetic analysis.

An important potential application of TRORD lies in the study of protein folding reactions. Jones et al. (1993) recently studied fast events in protein folding using laser photolysis and TROD techniques. The sensitivity of CD and ORD to secondary protein structure suggests that TRCD and TRORD could be powerful tools to study protein folding. A limitation in conducting spectral measurements in the peptide region is the large extinction of proteins in this region. The largest differences in CD between different secondary structures occur around 190 nm, whereas the largest differences in ORD are found around 200 nm (Geraci and Parkhurst, 1981; Imahori and Nicola, 1973). Most proteins absorb considerably less light at 200 nm than at 190 nm, giving ORD a better signal-to-noise advantage over CD. We are currently investigating methods for photogeneration of secondary structure changes in order to pursue TRORD studies of protein folding.

This work was supported by National Institutes of Health grant no. GM35158, awarded to D. S. Kliger. D. B. Shapiro would like to thank National Institutes of Health for their support through NRSA no. 1F32HL08969. R. M. Esquerra thanks the Patricia Harris Fellowship for support.

REFERENCES

Akesson, B., and P. Michelsen. 1981. Digestion and absorption of a sulphoxide analogue of triacylglycerol in the rat. *Chem. Phys. Lipids.* 29: 341–349.

Björling, S. C. 1991. Nanosecond time-resolved circular dichroism studies of proteins: photoinitiated processes in hemoglobin and phytochrome. Ph.D. dissertation, University of California, Santa Cruz.

Björling, S. C., C.-F. Zhang, D. L. Farrens, P.-S. Song, and D. S. Kliger. 1992. Time-resolved circular dichroism of native oat phytochrome photointermediates. *J. Am. Chem. Soc.* 114:4581–4588.

Björling, S. C., R. A. Goldbeck, S. J. Milder, C. E. Randall, J. W. Lewis, and D. S. Kliger. 1991. Analysis of optical artifacts in ellipsometric measurements of time-resolved circular dichroism. *J. Phys. Chem.* 95: 4685–4694.

Brodersen, S. 1990. The use of singular value decomposition in the fitting of molecular constants to spectroscopic data. *J. Mol. Spectrosc.* 142: 122–128.

Che, D., D. B. Shapiro, R. M. Esquerra, and D. S. Kliger. 1994. Ultrasensitive time-resolved linear dichroism spectral measurements using near-crossed linear polarizers. *Chem. Phys. Lett.* 224:145–154.

Chen, E., W. Parker, J. W. Lewis, P.-S. Song, and D. S. Kliger. 1993. Time-resolved UV circular dichroism of phytochrome A: Folding of the N-terminal region. *J. Am. Chem. Soc.* 115:9854–9855.

Devoe, H. 1964. Optical properties of molecular aggregates. II. Classical theory of the refraction, absorption, and optical activity of solutions and crystals. *J. Chem. Phys.* 41:3199–3208.

Djerassi, C. 1960. Optical Rotatory Dispersion. McGraw Hill, New York.

Einterz, C. M., J. W. Lewis, S. J. Milder, and D. S. Kliger. 1985. Birefringence effects in transient circular dichroism measurements with applications to the photolysis of carbonmonoxyhemoglobin and carbonmonoxymyoglobin. *J. Phys. Chem.* 89:3845–3853.

Evans, M. W. 1990. New non-linear circular birefringence effects of the electromagnetic field. *Phys. Lett. A.* 147:364–368.

Evans, M. W., S. Woznak, and G. Wagneriere. 1992. Field applied molecular dynamics (FMD) of circular dichroism and optical rotatory dispersion. *Physica B.* 179:133–156.

Gallop, P. M. 1957. Simplified formula for the operation of the Keston-type polarimeter. *Rev. Sci. Instr.* 28:209.

Geraci, G., L. J. Parkhurst, and Q. H. Gibson. 1969. Preparation and properties of α- and β-chains from human hemoglobin. *J. Biol. Chem.* 17: 4664–4667.

Geraci, G., and L. J. Parkhurst. 1981. Circular dichroism spectra of hemoglobins. *Methods Enzymol.* 76:262–275.

Goldbeck, R. A., T. D. Dawes, Ó. Einarsdóttir, W. H. Woodruff, and D. S. Kliger. 1991. Time-resolved magnetic circular dichroism spectroscopy of photolyzed carbonmonoxy cytochrome *c* oxidase (cytochrome aa_3). *Biophys. J.* 60:125–134.

Goldbeck, R. A., Ó. Einarsdóttir, T. D. Dawes, D. B. O'Connor, K. K. Sureras, J. A. Fee, and D. S. Kliger. 1992. Magnetic circular dichroism study of cytochrome ba_3 from *Thermus thermophilus*: Spectral contributions from cytochromes *b* and a_3 and nanosecond spectroscopy of CO photodissociation intermediates. *Biochemistry.* 31: 9376–9387.

Goldbeck, R. A., and D. S. Kliger. 1993. Nanosecond time-resolved absorption and polarization dichroism spectroscopies. *Methods Enzymol.* 226:147–177.

Golub, G. H., and C. Reinsch. 1970. Singular value decomposition and least squares solutions. *Numer. Math.* 14:403–420.

Hanspal, M., and G. B. Ralston. 1981. Purification of a trypsin-insensitive fragment of spectrin from human erythrocyte membranes. *Biochim. Biophys. Acta.* 669:133–139.

Henry, E. R., and J. Hofrichter. 1992. Singular value decomposition: applications to experimental data. *Methods Enzymol.* 210:129–192.

Hofrichter, J., J. H. Sommer, E. R. Henry, and W. A. Eaton. 1983. Nanosecond absorption spectroscopy of hemoglobin: Elementary processes in kinetic cooperativity. *Proc. Natl. Acad. Sci. USA.* 30: 2235–2239.

Hsu, M.-C., and R. W. Woody. 1969. Origin of the rotational strength of heme transitions in myoglobin. *J. Am. Chem. Soc.* 91:3679–3681.

Hsu, M.-C. and R. W. Woody. 1971. The origin of the heme Cotton effects in myoglobin and hemoglobin. *J. Am. Chem. Soc.* 93:3515–3525.

Huheey, J. E., E. A. Keiter, and R. L. Keiter. 1990. Inorganic Chemistry, Principles of Structure and Reactivity. Harper Collins College Publishers, New York. 499.

Imahori, K., and N. A. Nicola. 1973. Optical rotatory dispersion and the main chain conformation of proteins. *In* Physical Principles and Techniques of Proteins—Part C. S. J. Leach, editor. Academic Press, New York. 357–445.

Jensen, H. P., J. A. Schellman, and T. Troxell. 1978. Modulation techniques in polarization spectroscopy. *Appl. Spectrosc.* 32:192–200.

Jones, C. M., E. R. Henry, Y. Hu, C-K Chan, S. D. Luck, A. Bhuyan, H. Roder, J. Hofrichter, and W. A. Eaton. 1993. Fast events in protein folding initiated by nanosecond laser photolysis. *Proc. Natl. Acad. Sci. USA.* 90:11860–11864.

Keston, A., and J. Lospalluto. 1953. Simple ultrasensitive spectropolarimeters. *Fed. Proc.* 12:229.

Kliger, D. S., J. W. Kliger, and C. E. Randall. 1990. Polarized Light in Optics and Spectroscopy. Academic Press, Boston. 176.

Kliger, D. S., and J. W. Lewis. 1987. Recent advances in time-resolved circular dichroism spectroscopy. *Rev. Chem. Intermed.* 8:367–398.

Lewis, J. W., R. F. Tilton, C. M. Einterz, S. J. Milder, I. D. Kuntz, and D. S. Kliger. 1985. New technique for measuring circular dichroism changes on a nanosecond time scale. Application to (carbonmonoxy)-myoglobin and (carbonmonoxy)hemoglobin. *J. Phys. Chem.* 89: 289–294.

Lewis, J. W., R. A. Goldbeck, D. S. Kliger, X. Xie, R. C. Dunn, and J. D. Simon. 1992. Time-resolved circular dichroism spectroscopy: experiment, theory, and applications to biological systems. *J. Phys. Chem.* 96: 5243–5254.

Michl, J., and E. W. Thulstrup. 1986. Spectroscopy with Polarized Light. VCH, New York.

Milder, S. J., P. S. Weiss, and D. S. Kliger. 1989. Time-resolved absorption, circular dichroism, and emission of tRNA. Evidence that the photo-cross-linking of 4-thiouridine in tRNA occurs from the triplet state. *Biochemistry.* 28:2258–2264.

Milder, S. J., S. C. Björling, I. D. Kuntz, and D. S. Kliger. 1988. Time-resolved circular dichroism and absorption studies of the photolysis reaction of (carbonmonoxy)myoglobin. *Biophys. J.* 53:659–664.

Morris, N. P., S. L. Watt, J. M. Davis, and H. P. Bachinger. 1990. Unfolding intermediates in the triple helix to coil transition of bovine type XI collagen and human type V collagens $\alpha 1_2\alpha 2$ and $\alpha 1\alpha 2\alpha 3$. *J. Biol. Chem.* 265:10081–10087.

Moscowitz, A. 1962. Theoretical aspects of optical activity. *Adv. Chem. Phys.* 4:67–112.

Perutz, M. F., J. E. Ladner, S. R. Simon, and C. Ho. 1974. Influence of globin structure on the state of the heme. I. Human deoxyhemoglobin. *Biochemistry.* 13:2163–2173.

Poulsen, K. G. 1960. Evaluation of the Standard Model D Keston polarimetric attachment for the Beckman DU spectrophotometer. *Anal. Chem.* 32:410–413.

Rabinovitch, B., and M. Yamakawa. 1979. Optical rotatory dispersion and the Keston polarimetric accessory: a simplified method for use and calibration. *Anal. Biochem.* 92:55–60.

Spiro, T. G., G. Smulevich, and C. Su. 1990. Probing protein structure and dynamics with resonance Raman spectroscopy: cytochrome *c* peroxidase and hemoglobin. *Biochemistry.* 29:4497–4508.

Yip, S. K., and J. A. Sauls. 1992. Circular dichroism and birefringence in unconventional superconductors. *J. Low Temp. Phys.* 86:257–290.